



# Synthesis of W –TiO<sub>2</sub> nanoparticles for enhanced dye-sensitized solar cell performance

1- sajad Hosein Zadeh 2- Maryam Ghomashpasand

1- Guilan distribution company, Lahijan, sajadh89@yahoo.com

2-Department of Chemistry, Faculty of Science, University of Guilan, maryamm\_2001@yahoo.com

## Abstract

TiO<sub>2</sub> nanoparticles were prepared by sol-gel method by varying different mole % of tungsten and characterized by X-ray diffraction (XRD), scanning electron microscopy (SEM), energy dispersive spectroscopy (EDS), transmission electron microscopy (TEM). The energy-conversion efficiency of a cell based on 0.5 mol% W-doped TiO<sub>2</sub> is significantly better, compared to that of a cell based on undoped TiO<sub>2</sub>. The enhancement of the performance of DSSCs achieved using 0.5 mol% W–TiO<sub>2</sub> nanoparticle films is attributable to the slower recombination time and the introduction absorption of light in the visible range and especially in the range 300–420 nm. The above results demonstrate the potential application of introduction of W nanoparticles to improve for enhancing the performance of TiO<sub>2</sub> nanoparticle-based DSSCs, which can be produced on a large scale at low cost.

**Keywords:** Dye-sensitized solar cells, nanoparticles, W, TiO<sub>2</sub>,

## 1. Introduction

In recent years, Dye-sensitized nano-crystalline TiO<sub>2</sub> solar cell developed by Gratzel and his co-workers has attracted much attention due to its low cost and easy of fabrication [2]. It is well known that typical DSSCs consist of a TiO<sub>2</sub> photoanode with adsorbed dye molecules, a liquid electrolyte and a counter electrode [1-3]. Although TiO<sub>2</sub> nanoparticle electrodes have a large specific surface area which allows them to adsorb a sufficient number of dye molecules, electron transport in the TiO<sub>2</sub> nanoparticle network proceeds by a trap-limited diffusion process. The generated electrons in disordered TiO<sub>2</sub> nanoparticles travel through a large number of nanoparticles and boundaries before reaching the collecting electrode. Such a dynamic transit path of the electrons increases the chances of charge recombinations and thus decreases the efficiency of DSSCs [4-7]. Doping with the proper kind of metal ion could reduce the charge recombination and narrow the band gap of TiO<sub>2</sub>, thus broadening the width of absorption under sunlight. Then, the additional absorbed solar energy could increase the efficiency of the solar cells. Among these, W seems to be one of the most promising dopant in TiO<sub>2</sub> as it shifts the optical absorption spectrum towards the visible



range and improves the photocurrent density of TiO<sub>2</sub>. However, an excess of W leads to the recombination of charge carriers [8-10].

In this work, we have hydrothermally synthesized anatase TiO<sub>2</sub> nanoparticles as well as W–TiO<sub>2</sub> nanocomposites and have examined DSSCs made using these. The DSSCs made with W–TiO<sub>2</sub> nanoparticles are found to yield a much superior performance than the cells made with only TiO<sub>2</sub> nanoparticles. Various processes such as interfacial charge transfer and stability of interfaces can greatly influence the ability of a semiconductor–metal composite to sustain charge separation. We present results of different measurements and outline the possible origin of this effect.

## 2. Experimental

### 2.1. Materials

Titanium tetra isopropoxide (TTIP) glacial, Na<sub>2</sub>WO<sub>4</sub>·2H<sub>2</sub>O, chloroplatinic acid hexahydrate (H<sub>2</sub>PtCl<sub>6</sub>·6H<sub>2</sub>O) and acetic acid were purchased from Aldrich and used as received without further purification Sensitizing organometallic dye, cis-dithiocyanate-N,N'-bis-(4-arboxylate-4-tetrabutylammonium carboxylate-2,2'-bipyridine) ruthenium (II) (N719). and Fluorine-doped SnO<sub>2</sub> (FTO) electrode were purchased from Solaronix Co.

### 2.2. Preparation of a W–TiO<sub>2</sub> nanoparticles

Anatase TiO<sub>2</sub> nanocrystalline were prepared by means of microwave heating. In this method, 8 mL titanium isopropoxide was initially added to 15.5 mL glacial acetic acid with stirring. Next, 170 mL deionized water was added to the mixture dropwise with vigorous stirring. The solution was stirred for 1 h to get a clear transparent sol. Finally, the sol was placed under microwave irradiation (40% power) for 6 minutes. The white gel product was filtered, washed with deionized water and dried in oven for several hours. It was then calcined at 500 °C in air for 5 h at a ramp rate of 5 °C/ min. To prepare W-TiO<sub>2</sub>, the above procedure was repeated, including Na<sub>2</sub>WO<sub>4</sub>·2H<sub>2</sub>O (0.5 mol %) while adding water to the titanium isopropoxide mixture.

### 2.3. Fabrication of DSSC Cell

The FTO electrodes were washed with acetone, ethanol and deionized water in an ultrasonication bath for 15 min with a final wash in isopropanol. The TiO<sub>2</sub> and W–TiO<sub>2</sub> nanocomposite films were made by the doctor blade method and the films were then annealed at 450 °C for 30 min. For sensitization, the TiO<sub>2</sub> and W–TiO<sub>2</sub> nanocomposite films were impregnated with 0.5 mM N719 dye in ethanol for 24 h at room temperature. The sensitizer-coated TiO<sub>2</sub> films were washed with ethanol. The electrolytes were used with 0.6 M 1-hexyl-2,3-dimethylimidazolium iodide, 0.1 M LiI, 0.05 M I<sub>2</sub>, and 0.5 M 4-tert-butylpyridine in methoxyacetonitrile.

## 2.4. Characterization

The obtained powder were characterized by X-ray powder diffraction (XRD) using a D8 Bruker Advanced, X-ray diffractometer using Cu K $\alpha$ . radiation ( $\lambda = 1.54 \text{ \AA}$ ). The patterns were collected in the range  $2\theta=20\text{--}60^\circ$  and continuous scan mode. The morphology of as-prepared samples was observed using a scanning electron microscopy SEM (Philips XL30). The transmission electron microscopy (TEM) images of the powders was made in a Philips CM 10. The current density versus voltage (J–V) characteristics of the solar cell devices in the dark and under white light illumination were measured with an AM 1.5G solar simulator (300 W, Newport, USA) in  $100 \text{ mW/cm}^2$  conditions, adjusted with a standard PV reference cell (2 x 2 cm, a monocrystalline silicon solar cell, calibrated at NREL, Colorado, USA) with a Keithley 2400 source-measure unit.

## 3. Results and discussion

XRD patterns of various samples synthesized in the present investigation are shown in Figure 1. The XRD pattern corresponding to pure TiO<sub>2</sub>, Fig 1(a) was found to match with that of anatase phase (JCPDS No. 4-477). The W-doped sample also exhibit XRD pattern matching with single phasic anatase, with JCPDS No. 2-406. However, no peaks from any other impurities were observed, which indicate the high purity of the obtained pure and W-doped TiO<sub>2</sub>. The peaks corresponding to oxides of tungsten were not observed. Therefore, pure TiO<sub>2</sub> and the W substituted samples on calcinations at 500 °C for 5 h were found to retain anatase phase with no phase separation leading to rutile or WO<sub>3</sub> phase. Based on this, it can be inferred that either the entire tungsten has been substituted into the crystal lattice sites of the titania or it exists as WO<sub>3</sub> in a highly dispersed polymeric form over the titania surface. The average particle size was estimated by applying the Scherrer formula on the anatase (1 0 1) diffraction peak (the most intense peak):  $D = K\lambda/\beta\cos\theta$ , where D is the crystal size of the catalyst,  $\lambda$  the X-ray wavelength (1.54 Å),  $\beta$  the full width at half maximum(FWHM) of the catalysts,  $K = 0.89$  and  $\theta$  is the diffraction angle.

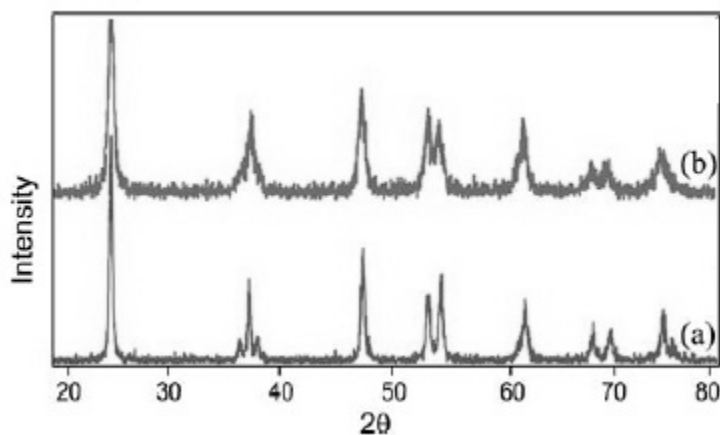


Fig. 1. XRD pattern of (a) pure nano TiO<sub>2</sub>, (b) 0.5% W-doped TiO<sub>2</sub>

Morphology of the pure and doped TiO<sub>2</sub> was determined by SEM micrographs. SEM micrographs of pure and W-doped nano TiO<sub>2</sub> are shown in Fig. 2. It can be seen that, an increase in doping tungsten leads to a smaller TiO<sub>2</sub> particle; it is also observed that nano TiO<sub>2</sub> are in pseudospherical shapes. All samples present strong agglomeration when they are seen by SEM, the morphology and particle size of them can not be resolved using this technique.

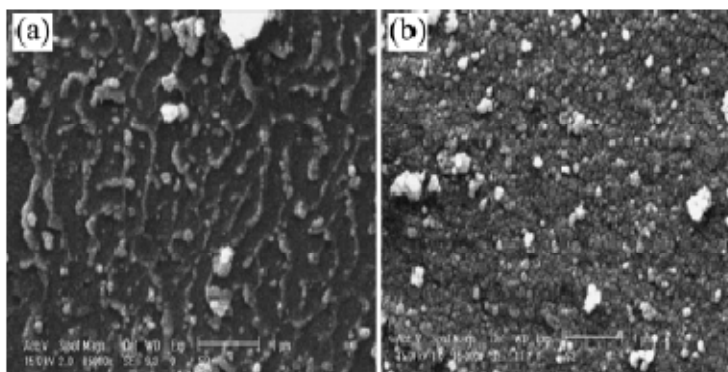


Fig. 2. SEM images of a) pure nano TiO<sub>2</sub>, (b) 0.5% W-doped TiO<sub>2</sub>

The EDX data of W (0.5% mol)-doped TiO<sub>2</sub> is shown in Fig. 3. Nano TiO<sub>2</sub> shows an intense peak around 4.5 keV. There are some tungsten peaks in the EDX pattern and this observation gave convincing evidence for the presence of tungsten on the surface of TiO<sub>2</sub>.

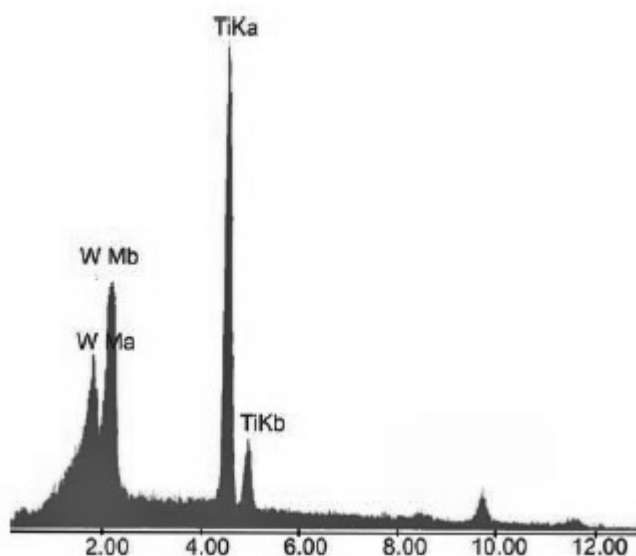


Fig. 3. EDX pattern of 0.5% W-doped TiO<sub>2</sub>

Fig. 4 displays transmission electron micrographs (TEM) of 0.5 mol % nanocrystalline TiO<sub>2</sub> of size 15 nm. It is observed from Fig. 5 that there is a significant decrease in the size of the nano powders with an increase in doping tungsten ion. Therefore, this result may be

attributed to the presence of tungsten component in the TiO<sub>2</sub> framework. Pure nanocrystalline TiO<sub>2</sub>, were largely distributed around 30-40 nm. On the other hand, the W-TiO<sub>2</sub>, was sharply distributed around 15-20 nm.

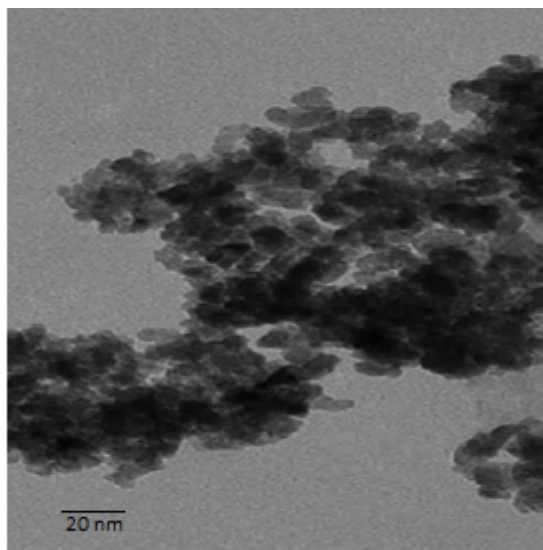


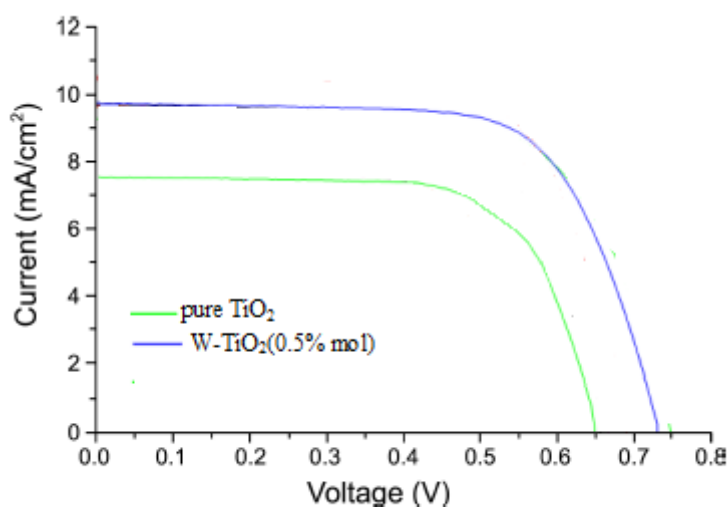
Figure 4. TEM images of 0.5% W-doped TiO<sub>2</sub>

The photoelectric properties were measured using a voltmeter and ampere meter (Model 2000, Keithley) with a variable load. A voltmeter above power failure and a lock-in amplifier were used. A 150 W illuminant Xenon lamp was employed as a radiation source at an AM-1.5 radiation angle. The light intensities were measured using a power analyzer and thermal smart-sensor. The FF and solar energy conversion efficiency ( $\eta$ ) were calculated according to Eqs. (1) and (2), respectively.

$$FF = I_{max} \times V_{max} / I_{sc} \times V_{oc} \quad (1)$$

$$\eta (\%) = P_{out} / P_{in} \times 100 = I_{max} \times V_{max} / P_{in} \times 100 = I_{sc} \times V_{oc} \times FF \quad (2)$$

Fig. 6 shows the photocurrent-voltage curves of the DSSCs assembled with the pure TiO<sub>2</sub> and the W-TiO<sub>2</sub>. The FF,  $V_{oc}$ ,  $J_{sc}$ , and overall energy efficiency were determined as described above. A DSSC assembled with pure TiO<sub>2</sub> had a  $V_{oc}$  of 0.65 V and a  $J_{sc}$  of 7.54 mAcm<sup>-2</sup> at an incident light intensity of 100 mW/ cm<sup>2</sup>. The power conversion efficiency was 3.1% for the pure TiO<sub>2</sub> anatase structure, but increased to 5.43% in the DSSC made from W-TiO<sub>2</sub> film, with a  $J_{sc}$  of 9.8 mAcm<sup>-2</sup> and a  $V_{oc}$  of 0.72 V.



sample	$V_{oc}$ (V)	$J_{sc}$ ( $mAcm^{-2}$ )	FF	Eff (%)
pure TiO <sub>2</sub>	0.65	7.54	0.56	3.1
W-TiO <sub>2</sub> (0.5% mol)	0.72	9.8	0.7	5.43

Fig. 6. I-V curves of the DSSCs fabricated with pure TiO<sub>2</sub> and W-TiO<sub>2</sub>(0.5% mol)

### Conclusion

In summary, the present results demonstrate the improvement in the photoelectric performance of DSSC by introducing tungsten into the TiO<sub>2</sub> photoanode. With 0.5 mol% of W dopant in the TiO<sub>2</sub> electrode, the light-to-electric conversion efficiency of the DSSC reaches 5.43% under a simulated solar light irradiation, which is enhanced by a factor of 2.33 compared to that of the DSSC fabricated with pure TiO<sub>2</sub>. Improvement of photovoltaic properties of DSSC by W-TiO<sub>2</sub> film photoanode is attributable to the strong absorption of dye and the high light harvesting efficiency, which can reduce the electron recombination loss and resulting in high conversion efficiency of the DSSCs.

### References

- [1] O'Rega B. n, and Graetzel M., "Low-cost, high efficiency solar cell based on dye-sensitized colloidal TiO<sub>2</sub> films", *Nature*, 353 ( 1991) 737-741.
- [2] Grätzel. M., "The advent of mesoscopic injection solar cells", *Progress in Photovoltaics: Research and Applications*, 14. (2006) 429-442.
- [3] Kuang D, Comte P, Zakeeruddin SM, Hagberg DP, Karlsson KM, Sun L. "Stable dye-sensitized solar cells based on organic chromophores and ionic liquid electrolyte", *Solar Energy* 85 (2011) 1189–94.
- [4] Du, L., Furube, A., Yamamoto, K., Hara, K., Katoh, R., Tachiya, M. "Plasmon-induced charge separation and recombination dynamics in gold-TiO<sub>2</sub> nanoparticle systems: dependence on TiO<sub>2</sub> particle size". *J. Phys. Chem. C* 113 ( 2009) 6454–6462.
- [5] Geetha M., Suguna K., Anbarasan P. M. "Photoanode Modification in DSSC Using Chromium Doped TiO<sub>2</sub> nanoparticles by sol-gel method", *Arch. Phy. Res.*, 2 (2014):303-308.



- [6] Xiang, Q., Yu, J., Cheng, B., Ong, H.C. "Microwave–hydrothermal preparation and visible-light photoactivity of plasmonic photocatalyst Ag–TiO<sub>2</sub> nanocomposite hollow spheres" Chem. Asian J. 5 (2010) 1466–1474.
- [7] Qi, J., Dang, X., Hammond, P.T., Belcher, A.M. "Highly efficient plasmon-enhanced dye-sensitized solar cells through metal@oxide core–shell nanostructure" ACS Nano 5 (2011) 7108–7116.
- [8] Fallah Shojaei A. and Loghmani M. "Effect of Microwave Irradiation on Morphology and Size of Anatase Nano Powder: Efficient Photodegradation of 4-Nitrophenol by W-doped Titania" Bull. Korean Chem. Soc. 33 (2012) 3981-3986.
- [9] Li M. "The research and development of Fe doped TiO<sub>2</sub>" Res. Mat. Sci. 2(2013) 28-33.
- Dhas, V., Muduli, S., Agarkar, S., Rana, A., Hannover, B., Banerjee, R., Ogale, S. " Enhanced DSSC performance with high surface area thin anatase TiO<sub>2</sub> nanoleaves" Solar Energy 85 (2011) 1213–1219.